IL NUOVO CIMENTO Vol. 37 C, N. 6 Novembre-Dicembre 2014
DOI 10.1393/ncc/i2015-11850-5

Colloquia: LaThuile14

Study of orbitally excited B mesons and evidence for a new $B\pi$ resonance

M. Kambeitz(*) for the CDF Collaboration

Institut für Experimentelle Kernphysik, Karlsruhe Institute of Technology (KIT) Karlsruhe, Germany

ricevuto il 31 Luglio 2014

Summary. — Analyzing the full CDF Run II data set of $9.6\,\mathrm{fb}^{-1}$, we find first evidence for a new resonance in $B^0\pi^+$ and $B^+\pi^-$ mass distributions with a significance of 4.4 standard deviations. We determine its mass, width, and relative production rate and refer to it as the $B(5970)$ state. Also, we present the first study of orbitally excited B^+ mesons and updated results on orbitally excited B^0 and B_s^0 mesons. We examine the B_1 and B_2^* states and measure masses, widths, their relative production rate, the branching fraction of the B_{s2}^{*0} state, and the production rate of the orbitally excited B^0 states relative to the B^0 ground state.

PACS 14.40.Nd – Bottom mesons.
PACS 13.25.Hw – Decays of bottom mesons.
PACS 12.40.Yx – Hadron mass models and calculations.

1. – Introduction

$B_{(s)}$ mesons consist of a $\overline{b}$ quark and a u or d (or s) quark. Studying their excitations supports the understanding of quantum chromodynamics by testing its low-energy approximations, such as the heavy quark effective theory (HQET) [1]. The ground state $B_{(s)}$ mesons and the spin-1 $B^*_{(s)}$ mesons have been thoroughly studied. The only known states beyond these two states, are the two orbitally excited states B_1 and B_2^* with orbital angular momentum $L = 1$ [2].

For each B^0, B^+, and B_s^0 meson, theory predicts four distinct $L = 1$ states, collectively referred to as $B^{**}_{(s)}$ mesons. Their dynamics is dominated by the coupling between the orbital angular momentum and the spin of the light quark combining to a total light-quark angular momentum $j = \frac{1}{2}$ or $j = \frac{3}{2}$, which is the analog to the fine-structure splitting in the hydrogen atom. Further splitting due to the spin of the $\overline{b}$ quark results

(*) E-mail: manuel.kambeitz@kit.edu

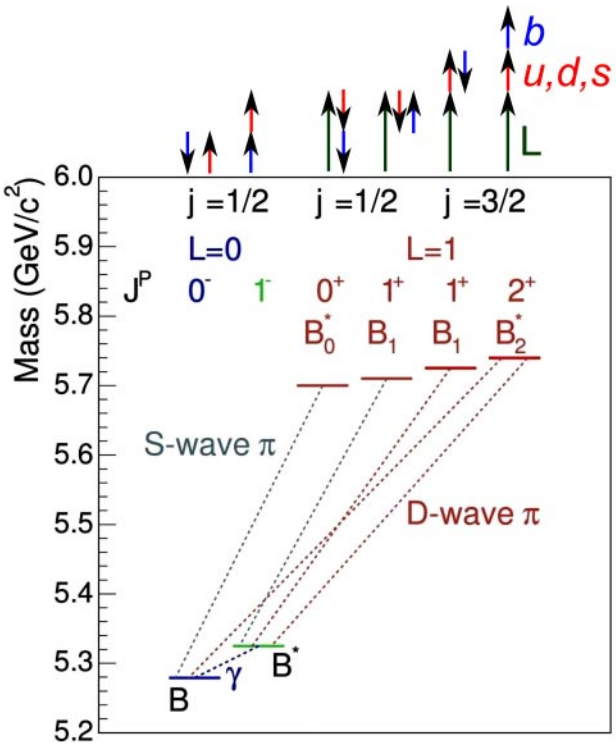

Fig. 1. – Spectrum and allowed decays for the lowest orbitally excited states $B^{**0,+}$. The alignment of the spins and orbital angular momenta is shown on top of the diagram. For B_s^{**0} mesons the pion is replaced by a kaon and the states have higher masses.

in two doublets of states: The $j = \frac{1}{2}$ states are named B_0^* and B_1 mesons; the states with $j = \frac{3}{2}$ are named B_1 and B_2^* mesons.

The spectrum and possible decays of $B^{**0,+}$ mesons are illustrated in fig. 1. They decay via the strong interaction to $B^{(*)}\pi$ combinations. $B^{**0,+}$ states with $j = \frac{1}{2}$ are expected to be too broad to be distinguishable from background at the CDF experiment. The $j = \frac{3}{2}$ states decay via a D-wave and are narrow enough to be observed at CDF. The B_2^* state can decay either to $B\pi$ or $B^*\pi$ final states. The low-energy photon from the $B^* \to B\gamma$ decay is typically not reconstructed; the decays of this state yield two structures in the $B\pi$ invariant mass spectrum. The B_1 state decays to $B^*\pi$. The orbital excitations of B_s^0 mesons are expected to have the same phenomenology as those of $B^{0,+}$ mesons, but different masses and widths. They decay to $B^{(*)0}\bar{K}^0$ and $B^{(*)+}K^-$ final states, but not to $B_s^0\pi^0$. Throughout this text, charge conjugate states are implied.

Orbitally excited B mesons were first observed in electron-positron collisions at LEP in 1995 [3-6] and further studied by the Tevatron experiments in proton-antiproton collisions [7-10]. Recent measurements were also performed by LHCb [11].

2. – Data sample and event selection

We use data from $p\bar{p}$ collisions at $\sqrt{s} = 1.96\,\text{TeV}$ at the Tevatron at Fermilab recorded by the CDF II detector. The data correspond to the full Run II integrated luminosity of

$9.6\,\mathrm{fb}^{-1}$. The key components of the CDF II detector [12] for this measurements are the charged-particle trajectory (tracking) subdetectors, namely the silicon-strip detector and the open-cell drift chamber, located in a uniform axial magnetic field of 1.4 T, together with the muon detectors. Additional information is obtained from time-of-flight detectors which are located outside the tracking detectors.

Recording of the events used in this measurement is initiated by two types of triggers. The J/ψ trigger is designed to record events enriched in $J/\psi \to \mu^+\mu^-$ decays by posing requirements on a di-muon system in the event. The displaced-track trigger [13] demands a pair of tracks with an intersection point displaced from the primary-interaction point and certain requirements on their impact parameter and transverse momentum, which preferentially selects events with decays of long-lived hadrons.

B mesons are formed in seven decay modes: $B^+ \to J/\psi K^+$, $B^+ \to \overline{D}^0\pi^+$, $B^+ \to \overline{D}^0\pi^+\pi^-\pi^+$, $B^0 \to J/\psi K^*(892)^0$, $B^0 \to J/\psi K^0_S$, $B^0 \to D^-\pi^+$, and $B^0 \to D^-\pi^+\pi^-\pi^+$. We reconstruct $B^{**}_{(s)}$ mesons in the $B^{**0} \to B^{(*)+}\pi^-$, $B^{**+} \to B^{(*)0}\pi^+$ and $B^{**}_s \to B^{(*)+}K^-$ channels. To improve the mass resolution, we use the Q value, defined as $Q = m(Bh) - m(B) - m_h$ instead of just $m(Bh)$, where $h = \pi$, K, to determine the resonance parameters because it reduces the effect of the B reconstruction resolution.

To the reconstructed data, we apply modest requirements on quantities providing significant signal-to-background separation. The resulting B mass distributions are then fit with a linear or exponential background model and one or two Gaussians as a signal model, depending on the B decay mode. This information is used to calculate ${}_s\mathcal{P}lot$ weights [14]. Observed events and their weights are input to a multivariate classifier [15], allowing training based on data only. Topological, kinematic, and particle identification quantities of the B mesons and their decay products are used as input variables. A moderate requirement is applied on the discriminator's output to remove candidates formed using random combination of tracks.

For the selection of $B^{**}_{(s)}$ mesons, we rely on simulations of $B^{**}_{(s)}$ decays. A neural network is trained to separate $B^{**}_{(s)}$ signal from background using simulations as signal and $B^{**}_{(s)}$ candidates observed in data, which contain besides background only a negligible signal fraction, as background. To avoid biasing the training to a certain mass range, simulated events are generated with the same Q-value distribution as the background in data.

The final selection is made by imposing a requirement on the output of the discriminator for each $B^{**}_{(s)}$ decay channel. For B^{**0} and B^{**+} candidates, the data sample is divided into a subsample with one candidate per event and a subsample with multiple candidates per event to increase sensitivity, due to the better signal-to-background ratio in the single-candidate subsample.

The resulting $B^{**}_{(s)}$-meson spectra are shown in fig. 2. The narrow state at the lowest Q value is interpreted as the $B_1 \to B^*h$ signal and the two higher Q-value structures as $B^*_2 \to B^*h$ and $B^*_2 \to Bh$ signals. At Q values around $550\,\mathrm{MeV}/c^2$ a broad structure is visible, in both the B^{**0} and B^{**+} invariant-mass distributions.

3. – Q-value fit

We use a maximum-likelihood fit of the unbinned Q-value distributions to measure the properties of the observed structures. Separate fits are performed for B^{**0}, B^{**+}, and B^{**0}_s mesons. For each flavor, the spectra for several B-meson decay channels are

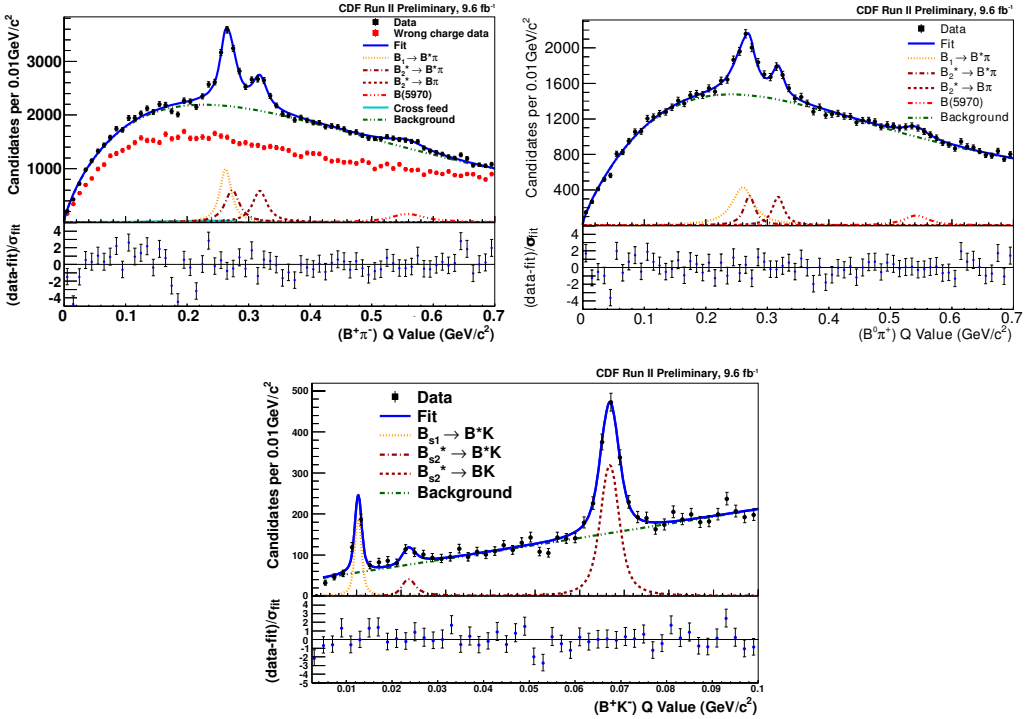

Fig. 2. – Distribution of Q-value of B^{**0} (top left), B^{**+} (top right) and B_s^{**0} (bottom) candidates. Data are summed over decay channels and overlaid with fit results. Also shown are deviations of data from the fit function, normalized to the fit uncertainty.

fit simultaneously. For the background component we use a Γ distribution [16] for the $B^{**0,+}$ spectra and a polynomial for the B_s^{**0} spectra. Each B signal is described by a Breit-Wigner shape whose parameters are free in the fit, convoluted with a double Gaussian that accounts for the detector resolution and whose parameters are determined from simulation. In order to determine directly the relative rates, the relative efficiencies for reconstructing the various $B_{(s)}^{**}$ states, determined from simulation, are included in the fit model. The structure in the $500 < Q < 600\,\mathrm{MeV}/c^2$ range of the spectrum is described by a Breit-Wigner function convoluted with a single Gaussian. In the B^{**0} fit, a component is added for misreconstructed B_s^{**0} mesons in which the low-energy kaon from the B_s^{**0} decay is reconstructed as a pion.

External inputs are used in the fit to resolve the ambiguity due to the overlapping $B^{**0,+}$ signal structures. The difference between the mean mass values of the $B_2^* \to Bh$ and $B_2^* \to B^*h$ signal structures is constrained to independent experimental measurements and the relative branching fraction of the $B_2^{*0/+}$ state is constrained by theoretical assumptions and measurements of the properties of D^{**} mesons.

To measure the relative rate of B and B^{**0} meson production, we use the ratio between the sum of B_1^0 and B_2^{0*} meson yields reconstructed in the $B^{**0} \to B^{+(*)}\pi^-$ decay, followed by the $B^+ \to \overline{D}^0\pi^+$ decay, and B^+ meson yields reconstructed in the same final state. The conditional probability for reconstructing a B^{**0} meson when a B^+ meson is already reconstructed in a $B^{**0} \to B^{(*)+}\pi^-$ event is determined from

simulation. Assuming isospin symmetry, we conclude that B^{**0} mesons decay to $B^{(*)0}\pi^0$ states in one third of the cases and are therefore not reconstructed.

4. – Systematic uncertainties

Several sources of systematic uncertainties are considered, including uncertainties on the absolute mass scale, mass resolution, and the fit model. Studies of the mass-scale uncertainty [8,9] and the detector resolution [17] have been performed in earlier analyses. The systematic uncertainty associated with possible mismodelings of the background shape is estimated by fitting with alternative background models. The lower bound of the B_s^{**0} fit is varied and the assumed photon energy from the B^* decay and the branching fraction of the B_2^* decays are varied within their uncertainties and the data are fit again. The deviations in the measured parameters with respect to the default results are taken as systematic uncertainties. Two broad $B^{**0,+}$ $j = \frac{1}{2}$ states are expected at similar masses as the two narrow $B^{**0,+}$ states and their influence to the measurement is estimated. The fitting procedure is tested for biases, by fitting random mass spectra with known signal parameters. An uncertainty is also assigned on the relative acceptance between $B_{(s)1} \to B^*h$, $B^*_{(s)2} \to B^*h$, and $B^*_{s2} \to Bh$ decays derived from simulation. The B^{**0}-meson yields in six independent ranges of transverse momentum in simulated events are compared to data and reweigted to estimate a systematic uncertainty on the conditional probability for reconstructing a B^{**0} meson when a B^+ meson is already reconstructed.

The dominant systematic uncertainty for most quantities is the description of the background shape, except for the Q values of the B_s^{**0} states, where the mass-scale uncertainty dominates. An additional significant contribution comes from the fit constraints, in which the B_2^* properties are less affected than those of the B_1, because the $B_2^* \to B\pi$ signal is well separated from the overlapping signals.

5. – Evidence for a $B(5970)$ state

As a consistency check, we apply to $B^+\pi^+$ combinations the same criteria as for the signal sample. No structure is observed in the invariant-mass distribution of the wrong-charge combinations as can be seen in fig. 2 (top left red squares). Due to neutral B meson oscillations, this cross check cannot be done with $\bar{B}^0\pi^+$ combinations.

The significance of the previously unobserved broad structure is determined by a p-value test. We consider the improvement in minimal logarithms of the likelihood ΔL between fits to data with $Q > 400\,\mathrm{MeV}/c^2$ that include or exclude the $B(5970)^{0,+}$ signal component. The background is described by a straight line. The signal yield is floating freely, and the mean and width are constrained to be in the ranges 450 to $650\,\mathrm{MeV}/c^2$ and 10 and $100\,\mathrm{MeV}/c^2$, respectively, to avoid having a large fraction of the signal outside the fit range. The $B(5970)^0$ and $B(5970)^+$ candidates are fit simultaneously with common signal parameters. The result of the fit to data is shown in fig. 3. Applying the same procedure to random distributions generated from the background distribution observed in the data, we find that we can exclude a random fluctuation at a statistical significance of 4.4σ.

To check the systematic effect of the background model on the significance, we repeat the significance evaluation with the default fit model of the $B^{**0,+}$ measurement and obtain a significance higher than 4.4σ.

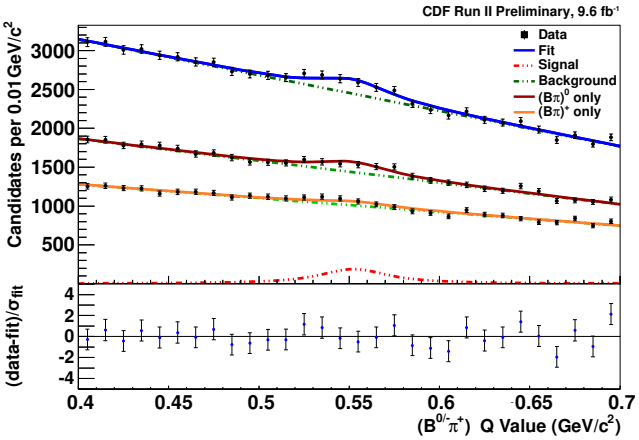

Fig. 3. – Sum of Q-value spectra of $B^{**0,+}$ candidates in all considered decay channels with fit results for the broad structure overlaid and the deviations of these from the fit function, normalized to the fit uncertainty.

6. – Results

We determine the properties of fully reconstructed B^{**0}, B^{**+}, and B_s^{**0} mesons shown in table I using about 8400 B^{**0} decays, 3300 B^{**+} decays, and 1350 B_s^{**0} decays.

The relative branching fractions of the B_{s2}^* state is found to be $\frac{\mathcal{B}(B_{s2}^*\to B^{*+}K^-)}{\mathcal{B}(B_{s2}^*\to B^+K^-)} = 0.11 \pm 0.03(\text{stat}) \pm 0.02(\text{syst})$.

We also determine how many narrow B^{**0} states are produced per B^+ meson for B^+ mesons having a transverse momentum larger than $5\,\text{GeV}/c$ and find a fraction of $19 \pm 2(\text{stat}) \pm 4(\text{syst})\%$.

The properties of the previously unobserved resonance in a sample containing 2600 $B(5970)^0$ and 1400 $B(5970)^+$ decays are shown in table I.

TABLE I. – *Measured masses and widths of $B_{(s)}^{**}$ mesons and the broad structure; and $r_{\text{prod}} = \frac{\sigma(B_1)}{\sigma(B_2^*)} \cdot \frac{\mathcal{B}(B_1\to B^*h)}{\mathcal{B}(B_2^*\to Bh)+\mathcal{B}(B_2^*\to B^*h)}$ which is relative production rates times branching fraction of $B_{(s)}^{**}$ mesons. The first contribution to the uncertainties is statistical; the second is systematic.*

	Q (MeV/c^2)	Γ (MeV/c^2)	r_{prod}
B_1^0	$262.6 \pm 0.8 \pm 1.3$	$20 \pm 2 \pm 5$	$0.66 \pm 0.12 \pm 0.51$
B_2^{*0}	$317.8 \pm 1.2 \pm 1.2$	$26 \pm 3 \pm 3$	
B_1^+	$261 \pm 4 \pm 3$	$42 \pm 11 \pm 13$	$1.8 \pm 0.9 \pm 1.2$
B_2^{*+}	$317.9 \pm 1.1 \pm 0.9$	$17 \pm 6 \pm 8$	
B_{s1}^0	$10.37 \pm 0.10 \pm 0.14$	$0.7 \pm 0.3 \pm 0.3$	$0.18 \pm 0.02 \pm 0.02$
B_{s2}^{*0}	$66.75 \pm 0.13 \pm 0.14$	$2.0 \pm 0.4 \pm 0.2$	
$B(5970)^0$	$558 \pm 5 \pm 12$	$70 \pm 18 \pm 31$	
$B(5970)^+$	$541 \pm 5 \pm 12$	$60 \pm 20 \pm 40$	

We measure the rates of the broad structures relative to the decays $B_2^* \to B\pi$ in the range $p_T > 5\,\mathrm{GeV}/c$ of the produced B meson to be $r'_{\mathrm{prod}}(B(5970)^0) = 0.5 \pm 0.1(\mathrm{stat}) \pm 0.3(\mathrm{syst})$ and $r'_{\mathrm{prod}}(B(5970)^+) = 0.7 \pm 0.2(\mathrm{stat}) \pm 0.8(\mathrm{syst})$, defined as $r'_{\mathrm{prod}}(B(5970)) = \frac{\sigma(B(5970))}{\sigma(B_2^*)} \frac{\mathcal{B}(B(5970)\to B^{(*)}\pi)}{\mathcal{B}(B_2^*\to B\pi)}$.

7. – Summary

Using the full CDF Run II data sample, we perform a study of excited $B_{(s)}$ mesons. We measure the masses and widths of the narrow $B_{(s)}^{**}$ states. For the first time, we observe exclusively reconstructed B^{**+} mesons. Also for the first time, the width of the B_1^0 state is measured. The results are consistent with and more precise than previous determinations based on a subset of the present data [8, 9]. The results are also generally compatible with determinations by the D0 [7] and LHCb experiments [11], with the exception of the mass difference between B_1^0 and B_2^{0*} mesons measured by the D0 experiment. The properties of the B^{**0} and B^{**+} states are consistent with isospin symmetry.

We find evidence with a significance of 4.4σ for a previously unseen charged and neutral $B\pi$ signal. Interpreting it as a single state, we measure its properties for charged and neutral combinations and call it $B(5970)$. The properties of the new states are statistically consistent as expected by isospin symmetry.

REFERENCES

[1] Isgur N. and Wise M. B., *Phys. Lett. B*, **232** (1989) 113; **237** (1990) 527.
[2] Beringer J. *et al.* (Particle Data Group), *Phys. Rev. D*, **86** (2012) 010001 and 2013 partial update for the 2014 edition.
[3] Abreu P. *et al.* (DELPHI Collaboration), *Phys. Lett. B*, **345** (1995) 598.
[4] Akers R. *et al.* (OPAL Collaboration), *Z. Phys. C*, **66** (1995) 19.
[5] Buskulic D. *et al.* (ALEPH Collaboration), *Z. Phys. C*, **69** (1996) 393.
[6] Barate R. *et al.* (ALEPH Collaboration), *Phys. Lett. B*, **425** (1998) 215.
[7] Abazov V. M. *et al.* (D0 Collaboration), *Phys. Rev. Lett.*, **99** (2007) 172001.
[8] Aaltonen T. *et al.* (CDF Collaboration), *Phys. Rev. Lett.*, **102** (2009) 102003.
[9] Aaltonen T. *et al.* (CDF Collaboration), *Phys. Rev. Lett.*, **100** (2008) 082001.
[10] Abazov V. M. *et al.* (D0 Collaboration), *Phys. Rev. Lett.*, **100** (2008) 082002.
[11] Aaij R. *et al.* (LHCb Collaboration), *Phys. Rev. Lett.*, **110** (2013) 151803.
[12] Acosta D. *et al.* (CDF Collaboration), *Phys. Rev. D*, **71** (2005) 032001.
[13] Abulencia A. *et al.* (CDF Collaboration), *Phys. Rev. Lett.*, **96** (2006) 191801.
[14] Pivk M. and Francois R. Le Diberder, *Nucl. Instrum. Methods A*, **555** (2005) 356.
[15] Feindt M. and Kerzel U., *Nucl. Instrum. Methods A*, **559** (2006) 190.
[16] Hazewinkel M. (Editor), *Encyclopaedia of Mathematics* (Springer) 1994.
[17] Aaltonen T. *et al.* (CDF Collaboration), *Phys. Rev. D*, **84** (2011) 012003.